Chapter 1 Introduction

1.1 Introduction

One of the characteristic chemical functions of metal ions and/or their complexes is their specific and reversible binding ability with small molecules, such as alkene, carbon monoxide, molecular nitrogen, and molecular oxygen.[1-3] For instance, ethylene coordinatively binds with silver or copper ions and molecular oxygen with metalloporphyrin. When such metal ions or metalloporphyrins are molecularly bound in macromolecules to form metal complexes, the reversible binding of small molecules with the metal complexes in macromolecules offers extensive potential applications, such as separation membranes, absorbents, and sensors.

A macromolecule provides a suitable functional group for either complexation with metal ions of metal salts or attaching metal complexes into the macromolecular matrix through a coordination bond; typical examples of the former are silver-polymer complexes, while cobalt porphyrins incorporated on a polymer backbone through coordination bonding are examples of the latter.

Since the structure and properties of metal complexes in macromolecules are affected by the surrounding macromolecules,[4,5] metal complexes in macromolecules exhibit characteristic behavior in binding reactions with small or gaseous molecules as well as unique chemical reactivities and physiochemical properties. When a small molecule contacts with metal complexes in a macromolecular matrix, it is dissolved in the macromolecule as a result of coordinative binding with the metal complex if there is a specific interaction between the small molecule and the metal complex. In many cases, such as a silver-polymer complex with olefin or a metalloporphyrin with oxygen, the binding is reversible and specific, resulting in an enhanced total solubility and transport. Since small molecular binding to metal complexes is a simple phenomenon or elementary step without any further reaction involved, monitoring the adduct formation and transport of small gaseous molecules in macromolecules containing a metal complex is a simple but powerful tool to characterize the reactivity and functionality of metal complexes in macromolecules.

In organometallic chemistry, complexes between metal salts and olefins, such as Zeise's salt, have been identified since the early 19th century. Silver or copper ions are known to form a reversible adduct with olefins.[6,7] The bond between the olefin molecule and the metal ion is regarded as a dative σ bond to a suitable hybrid orbital

of the metal (*s* or *sp* in silver ion). This bond is analogous to the dative carbon-metal σ bond between carbon monoxide and transition metals and metal-carbon (antibonding orbital) π bond by back-donation (Figure 1-1).[6,7]

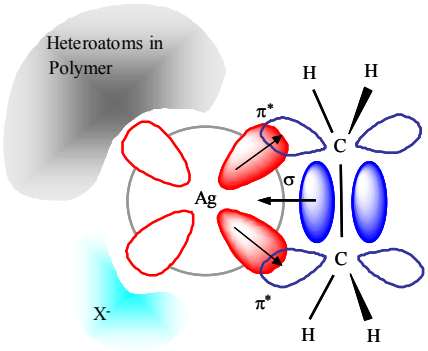

Figure 1-1. Bonding interaction between silver ion and olefin.

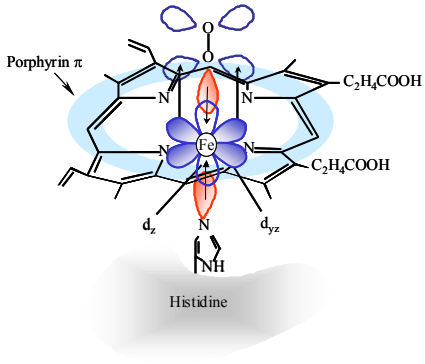

Figure 1-2. Oxygen binding in hemoglobin/myoglobin.

The reversible binding behavior between silver ions and olefins can be utilized to separate unsaturated hydrocarbons (olefins) from saturated ones (paraffins).[8] The extent and reversibility of the bonding between silver ions and olefins vary depending on the structure of the olefin and type of macromolecule. Therefore, the binding ability and its reversibility for specific applications can be tailored using macromolecular ligands. The roles of the macromolecule (polymer) surrounding the central silver ion are as follows: first, tuning the strength of the binding between the silver ion and the olefin, second, providing a hydrophobic environment through the formation of a micro-domain, third, prolonging the life-time of the metal complexes by immobilizing the silver ions, and fourth, feasibility in fabricating various forms including films, beads, and so on.

A similar binding of small molecules is also observed in iron and cobalt porphyrins.[2,3,1-10] Iron (II), d^6, and cobalt(II), d^7 are not particularly soft metal cations, yet the "softening" (symbiotic) action of the tetrapyrrole ring system in metalloporphyrin enables molecular oxygen binding. The porphyrins contain a highly resonant planar ring system in which four nitrogen atoms are fixed in the center at a spacing that is ideal for their unshared electrons to bond with a metal ion. The iron porphyrin group has attracted the most attention because it plays a central biological role in the binding of molecular oxygen, O_2. In a living body, oxygen is transported or stored with the help of hemoglobin or myoglobin. Iron(II) ions have a coordination number of six. When a ferrous ion forms a chelate with a porphyrin, two of its coordination sites are still unfilled. Therefore, one of the functions of the polypeptide chain of hemoglobin and myoglobin is to provide a histidyl residue as a position where

one of the nitrogen atoms links to the fifth coordination position of the iron ion, as shown in Figure 1-2.

In this chapter, the specific and reversible bindings of small molecules with metal complexes in macromolecules are described using the examples of silver-polymer complexes and metalloporphyrins coordinatively bound in macromolecules. Next, their structures are characterized, followed by potential applications as a gas-separation membrane and gas-carrying material.

1.2 Binding of Small Molecules to Metal Complexes in Macromolecules

1.2.1 Formation of Silver Polymer Complexes

Polymer complexes are composed of a metal complex bound to a chain of a linear macromolecule via a Type I coordinative bond. The formation process of metal-polymer complexes can be schematically written as in Eq 1-1, where M and X are a metal ion and its counter anion, respectively.

(1-1)

The complexation process in a solid state involves the dissociation of metal salts into ions (losing lattice energy) and the coordination of the cation to a heteroatom (or polar group) of a macromolecule (gaining coordination bonding or complexation energy). It is known that the lower the lattice energy, the easier it is to make metal-polymer complexes. Thus, the lattice energy is one important criterion in forming metal-polymer complexes. The complexation energy is associated with the coordinative interaction between the metal cation and the polar groups in the polymer backbone. For example, polar oxygen or nitrogen atoms coordinate with transition metal cations, resulting in the homogeneous complexation of the metal cations into a polar macromolecular matrix. Specifically, oxygen atoms from an ether or amide group in poly(ethylene oxide) (PEO), poly(2-ethyl-2-oxazoline) (POZ), or poly(N-vinylpyrrolidone) (PVP) coordinate with silver cations to form silver-polymer complexes.[12,13] The structures of the repeat unit of the polymers are presented in Figure 1-3. The significance of silver-polymer complexes was already discussed in the Introduction.

When silver ions are coordinated by heteroatoms in a polymer matrix to form polymer complexes, their structure and properties will be changed mainly due to the

coordinative interaction between the silver ions and polar groups in the polymers. This change in structure can be seen clearly by the variation of the intersegmental distance and glass transition temperature (T_g) of the silver-polymer complex. The intersegmental distance and d-spacing, were determined using wide angle X-ray scattering (WAXS) based on Bragg's law. In a WAXS study, the first broad maximum peak for $AgCF_3SO_3$-POZ complexes was assigned to the interchain distance and decreased with the silver concentration at low silver concentrations regime; the silver ions become a transient crosslinker and pull the polymer chains by coordinative interaction, thereby decreasing the interchain distance.

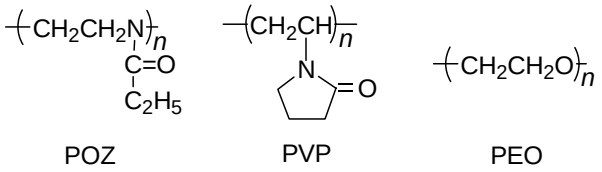

Figure 1-3. Structure of the polymers POZ, PVP, PEO.

The T_g of the silver-POZ complex initially increases with the silver concentration, reaches a broad maxima, then slightly decreases again. The increase in T_g with the complexation of the silver ions is primarily attributable to both the reduced chain mobility in the transient cross-links of the polymer segments due to the silver cations and the dangling of silver cations on the polymer chain.[14]

Gas permeability is also one of the parameters used to detect a change in the structure of a polymer. Since paraffins, such as propane, do not have any specific interaction with silver ions and thus only permeate via normal sorption and diffusion transport, the permeance behavior of propane is mostly determined by the microstructure and chain mobility of a polymer complex. As such, the propane permeances of POZ films decrease rapidly with $AgCF_3SO_3$, which is consistent with the results of the d-spacings and glass transition temperatures.

Metal ion complexations affected the structure and physicochemical properties of polymer-ligands, which is generally observed in metal-polymer complexes, for example, Li-polymer complexes (electrolytes).

1.2.2 Olefin Binding and Reversibility

When small molecules, such as olefins, come into contact with a metal complex in macromolecules, such as silver-polymer complexes, a significant amount of olefins are absorbed in the silver-polymer complexes. The propylene solubilities in Ag-POZ complex films ([Ag^+] in $AgBF_4$: [C=O] in POZ = 1:1, ca. 80 wt-% of $AgBF_4$ in the polymer matrix) were plotted against the propylene pressure, as shown in Figure 1-4.[15] The propylene solubility in pure POZ was very small. However, the propylene

solubilities in a 1:1 $AgBF_4$-POZ complex (190 cm^3(STP) and 240 of propylene per 1 cm^3 of silver-polymer complex at 50 and 190 kPa, respectively) significantly increased ca. 100 times compared to those in pure POZ because of the chemically specific binding of propylene into silver ions.

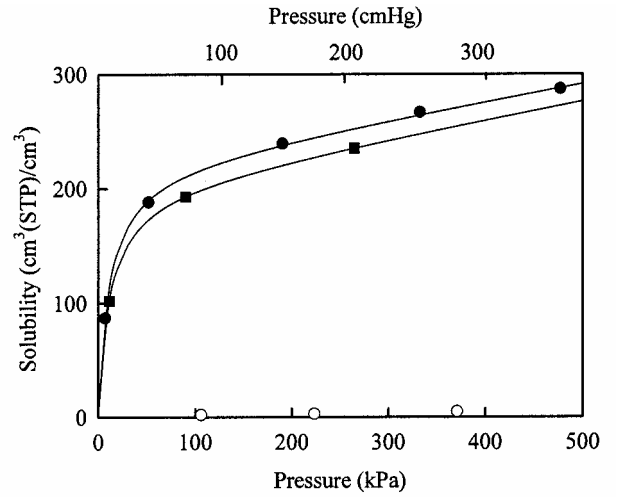

Figure 1-4. Solubility of propylene in solid silver-polymer complex films at 25°C.[15] $[Ag^+]$:[C=O] = 1:1. ●:$AgBF_4$-POZ; ■: $AgBF_4$-PVP; ○:pure POZ. The propylene solubility in pure PVP film was immeasurably small and was not plotted in the figure.

Propylene dissolves in two modes, a physical dissolution mode in the matrix and a binding mode resulting from a reversible chemical reaction with metal complexes. Henry's law commonly expresses the physical dissolution mode for small molecules, while the Langmuir model adequately describes the reversible binding mode, as written in Eq. 1-2. Mathematically, a Langmuir adsorption isotherm for a small molecule in a porous media is identical to the expression of the olefin concentration bound to the metal complex.

$$Ag^+(\text{polymer}) + \text{olefin} \rightleftharpoons \text{olefin} - Ag^+(\text{polymer}) \qquad (1\text{-}2)$$

$$K = \frac{[\text{Ag} - \text{olefin}]}{[Ag^+][\text{olefin}]} \qquad (1\text{-}3)$$

The total solubility is the summation of the contributions of both the dissolution mode based on Henry's law and the binding mode using the Langmuir model: the dual mode sorption.[11] At equilibrium, the total solubility of olefin becomes Eq. 1-4, where C is the total concentration of the olefin gas absorbed in the sample, p is the applied olefin pressure, k_D is the solubility coefficient of the olefin gas for Henry's law mode, K is the olefin binding equilibrium constant of Eq. 1-2, as defined in Eq. 1-3, and C_c is the saturated amount of the olefin gas bound to the silver complex.

$$C = k_D p + \frac{C_c K p}{1 + K p} \quad (1\text{-}4)$$

The propylene solubilities are analyzed using the dual sorption model in Eq. 1-4 and the parameters are listed in Table 1-1. The k_D value is very small and represents a small physical dissolution term, which only contributes 7 % to the total solubility at 100 kPa, whereas the binding Langmuir term provides a major contribution represented by a large C_c value of 220 (cm^3(STP)/cm^3) and large K value of 0.12 (1/cmHg) in comparison with 0.06 for the oxygen binding to the picketfence cobalt porphyrin-OPy membrane (see Figure 1-10), representing the strong affinity of propylene to a silver complex. These results indicate that the total solubility mostly depends on the binding of propylene by a reversible chemical reaction between the propylene and the silver complex in the polymer.

Table 1-1. Binding equilibrium constant (K), solubility coefficient (k_D), and saturated amount of the gas bound to the silver complex (C_c) of the solid silver-POZ complex for propylene.[16]

	$AgBF_4$-POZ	$AgCF_3SO_3$-POZ
k_D (cm^3(STP)/ cm^3 cmHg)	0.20	0.20
K (1/cmHg)	0.12	0.04
C_C (cm^3(STP)/cm^3)	222	131

The olefin solubility in a silver-PEO complex has been also reported. $AgBF_4$-PEO absorbed 45 cm^3(STP) of propylene per 1 g of silver-PEO complex, at 30 ^oC and 93 kPa.[17] The relationship between the olefin solubility and the structure can be understood by an *ab initio* calculation based on the density function theory of the model system. The theoretical calculation shows that the bond length between the silver ion and the closest anion atom in the $AgBF_4$-PEO film changes from 2.309 to 2.506 Å with the addition of ethylene, and the free energy ΔG for the formation of an ethylene adduct with $AgBF_4$ is favorable for an ethylene-silver complex in PEO[15,18,19] (Figure 1-5).

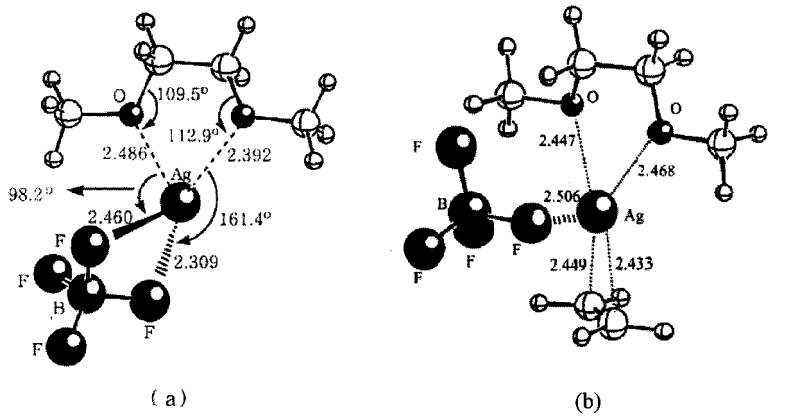

Figure 1-5. Structures of complexes of (a) $AgBF_4$-1,2-dimethoxy ethane complex, (b) $AgBF_4$-1,2-dimethoxy ethane-ethylene adduct where 1,2-dimethoxy ethane is a model compound of poly(ethylene oxide).[15] The silver ion is coordinated by two oxygen atoms from 1,2-dimethoxy ethane and two F atoms from the anion to make silver-polymer complexes, when $AgBF_4$ is complexed with 1,2-dimethoxy ethane. One of the two F atoms bound to the silver ion is replaced by an ethylene molecule, when one ethylene molecule approaches to the complex under ethylene environment.

The reversible olefin binding to silver ions in solid polymer complexes was investigated using FTIR and UV/vis spectroscopies (for an experiment see chapter 9.5.1).[20-22] The series of IR spectra in Figure 1-6 demonstrate the reversible olefin coordination to the silver-poly(vinylmethylketone) (PVMK) complex.[21] The free C=O stretching peak at 1709 cm^{-1} shifts to a lower frequency due to the silver complex formation, as shown in Figure 1-6a, demonstrating the coordination of carbonyl groups to silver ions. A silver-PVMK complex film ([Ag^+] in $AgBF_4$:[C=O] in PVMK = 1:2; 58 wt% of $AgBF_4$ in the polymer metrix) only showed a coordinated C=O peak at 1681 cm^{-1}, implying that all the carbonyl oxygen is coordinated to silver ions. When the sample was exposed to 207 kPa of propylene, then purged with nitrogen gas to sweep up any excess propylene, a new peak appeared at 1586 cm^{-1} (Figure 1-6c). This new peak represents the C=C stretching vibration of the coordinated propylene (cf. $\nu_{C=C}$ of free 1-hexene = 1640 cm^{-1}). It is important to note that the peak at 1586 cm^{-1} remains even after out-gassing at 10^{-5} torr and room temperature for 4 hrs. However, the exposure of the propylene coordinated complex to 207 kPa of 1,3-butadiene and subsequent purging with nitrogen produced a new peak at 1558 cm^{-1} with the concomitant disappearance of the peak for the coordinated propylene at 1586 cm^{-1}. The peak at 1558 cm^{-1} represents the C=C stretching frequency of the coordinated 1,3-butadiene (Figure 1-6d). The peak at 1558 cm^{-1} was again replaced by a peak at 1586 cm^{-1} with the re-introduction of propylene into the silver-PVMK complex previously

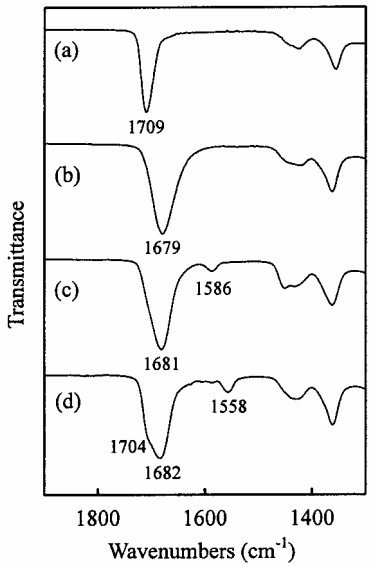

Figure 1-6. IR spectra for the solid state interactions of the silver-PVMK complex and olefins: (a) PVMK, (b) $AgBF_4$-PVMK ($[Ag^+]$:[C=O] = 2:1), (c) propylene-coordinated film and (d) 1,3-butadiene-coordinated film.[21]

coordinated with 1,3-butadiene.

This reversible olefin coordination can also be observed based on spectral changes in the UV absorption spectra.[21] A strong and broad absorption band at 220 – 230 nm for the propylene coordinated with the $AgBF_4$-PVMK complex ($[Ag^+]$:[C=O] = 2:1) disappeared and a new band appeared at around 258 nm for the coordinated 1,3-butadiene when the propylene coordinated film was exposed to a 1,3-butadiene atmosphere and followed by a nitrogen gas purge. The absorption band of the coordinated propylene at 220 – 230 nm reappeared when propylene is introduced into the cells containing the 1,3-butadiene coordinated film.

Because the concentration of the metal complex moiety in the polymer domain of a solid-state film is higher than that of a homogeneously solubilized complex in solution, even a simple spectrophotometer is effective for observing the gaseous molecule-binding reactions and ligand-bonding characteristics of complexes.

Both of IR and UV spectroscopy indicate that coordinated propylene is labile enough to be easily replaced by other olefins. The rapid exchange reaction seems to be a determining factor for olefin transport and a driving force for olefin-facilitated transport.

1.2.3 Formation of Metalloporphyrin-Polymer Complexes

Polymer complexes of metalloporphyrins are formed by mixing solutions of a polymer-ligand with a metalloporphyrin, as schematically written in Eq. 1-5, where M,

L, and the square of dashed lines are a metal ion, such as iron or cobalt ion, a nitrogenous residue of a polymer-ligand, and a porphyrin planar ring, respectively.

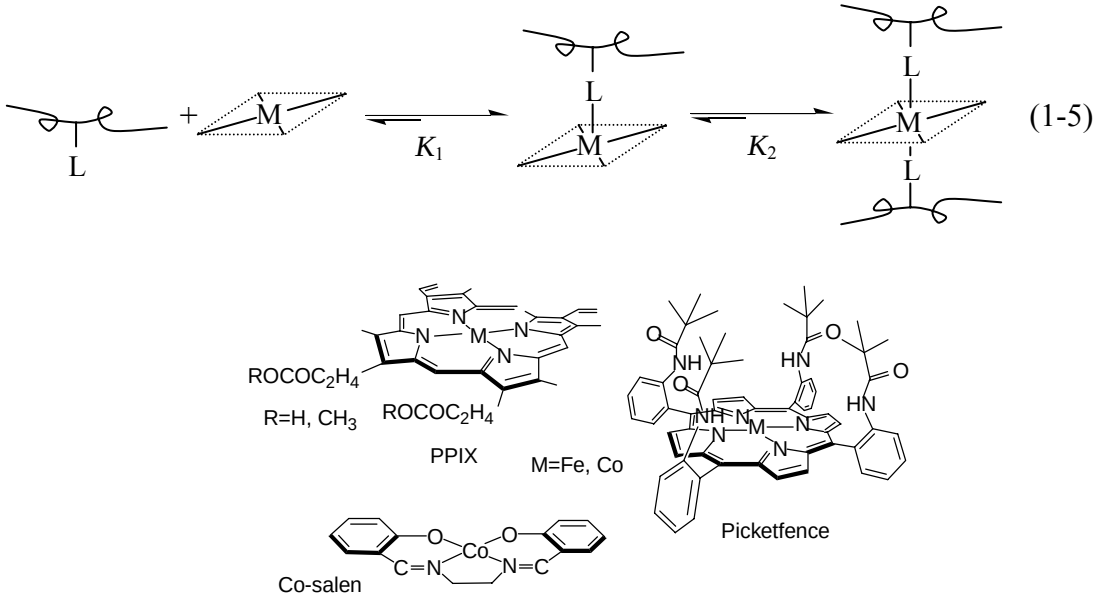

Figure 1-7. Examples of porphyrins.

Typical examples of metalloporphyrins and polymer-ligands are presented in Figures 1-7 and 1-8, respectively. Other metalloporphyrin-related complexes include metallophthalocyanines and cobalt Schiff's base chelate: the latter (Co-salen) is given in the bottom of Figure 1-7. A polymer-ligand is made to coordinate to a vacant site or the fifth coordination position of the complex. The ligand-coordination in the pendant-type metalloporphyrin enables the formation of an oxygen-adduct, as represented in Figure 1-7. However, when the polymer-ligand further coordinates to the sixth coordination position of the metalloporphyrin, as shown in Eq. 1-5, the metalloporphyrin loses its oxygen-binding ability. Consequently, the structure and hence the functions of a metalloporphyrin are significantly affected by the attachment of a polymer-ligand.

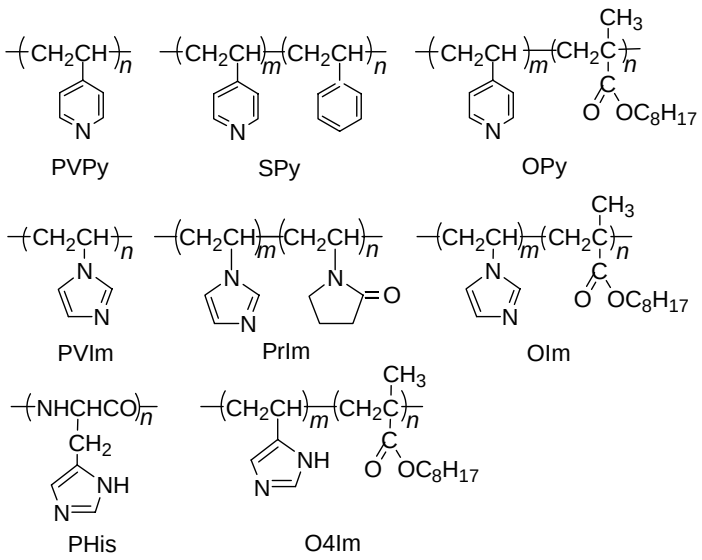

Figure 1-8. Examples of polymer ligands.

For a reversible oxygen-binding, the oxidation potential of a metalloporphyrin must be within a range such that a certain amount of electron density is located in the bound oxygen molecule, yet not so great that irreversible oxidation of the metal accompanying the formation of a super oxide anion ($O_2^{-\bullet}$) occurs[10,23,24] (Figure 1-2). Iron(II) and cobalt(II) ions often satisfy this first requisite. An aromatic and nitrogenous ligand, such as imidazole and pyridine, contributes to this requisite, from the viewpoint of an axial ligand of a metalloporphyrin. The coordination number of one or two, that is, the molar ratio of the coordinated axial ligand to the metal ion of porphyrin (Eq. 1-5), and the formation constants of metalloporphyrin-polymer complexes have been well studied by spectroscopic titration.[4] In solutions, the coordination number is one to preferentially form five-coordinate metalloporphyrin complexes with a K_1 value of $10 - 10^3$ M^{-1} for almost all imidazole and pyridine-based ligands. In the case of cobalt porphyrin, the K_2 value for a six-coordinate complex is very small <1 M^{-1},[25] and the cobalt porphyrin hardly form a six-coordinate porphyrin complex. But, the K_2 value for a six- coordinate ironporphyrin is a competitive value to that of the five-coordinate's K_1. In the procedure, for example, casting or evaporating its solution to yield a solid sample of metalloporphyrin-polymer complex, the solution turns highly concentrated; the formation of six-coordinate metallo(especially iron) porphyrin complexes, which is no more active in oxygen-binding, becomes not negligible.

ESR spectroscopy is effective for determining such coordination structure for cobalt(II) and iron(III) porphyrins.[25] For example, the ESR parameters; $g_\perp$= 2.3 and

$g_{//}$= 2.0: Both signals split into hyperfine lines due to the ^{59}Co nucleus, and several of the parallel signals were further spilt into equal intensity super-hyperfine lines. The latter was derived from the nitrogen nucleus of the nitrogenous ligand at the fifth coordination site of a cobalt porphyrin.

The effects of polymer-ligands in the complexation with a metalloporphyrin have been compared with those of the corresponding monomeric ligands. The formation constants K_1 of metalloporphyrin-polymer complexes are $10 - 10^2$ times larger than those of monomeric complexes in a solution.[4] This phenomenon appears to be general for metal-polymer complexes, and can be explained by assuming that the concentration of the ligand is locally higher in the domain of a polymer-ligand. This stability in the complexation provides an advantage for polymer complexes that minimal excess feeding of a polymer-ligand to a metalloporphyrin establishes the formation of a complex in both solution and solid states.

Apart from the coordinative bond, an electrostatic or hydrophobic interaction between a metalloporphyrin and a polymer-ligand also plays a role in the complexation, especially in an aqueous solution.[4] It is well known that metalloporphyrins easily aggregate in a solution (and even in a solid state) based on a stacking interaction. The dispersion effects of polymers on porphyrin aggregation have been reported. For example, aggregated iron protoporphyrin IX (PPIX, M = Fe and R = H in Figure 1-7) is effectively dispersed by a copolymer of vinylimidazole and vinylpyrrolidone (PrIm in Figure 1-8), which is a water-soluble but hydrophobic polymer-ligand. Ironporphyrin is dispersed by the hydrophobic effect of a polymer-ligand and/or tightly coordinated on a polymer-ligand matrix to prevent aggregation. The secondary structure effect of a polymer-ligand has been also studied; poly(L-histidine) (PHis in Figure 1-8) has a α-helical conformation that yields a six-coordinate iron PPIX complex with large K_2 values.

Casting the complex solution of a metalloporphyrin and a polymer-ligand such as poly (vinylimidazole-*co*-alkylmethacrylate) (OIm in Figure 1-8), for example, on a Teflon plate and drying, yielded both a homogenously dispersed metalloporphyrin in a solid state and a mechanically tough membrane.[26] The T_g of the membrane was increased, for example, from -1^{o}C for the OIm itself to 6 ^{o}C and the membrane became brittle after the 40 wt% -incorporation of cobalt porphyrin; this was explained by the stiffening effect of the incorporated planar and rigid porphyrin molecules on the segmental motion of the polymer chains. The chemical structure of a polymer-ligand has to be carefully designed to obtain a solid membrane of metalloporphyrin-polymer complexes that is feasibly applicable to gas permeation experiments.

The membrane was homogenously and deeply red in color with a metalloporphyrin. X-Ray diffractometry of the membrane provides no significant pattern, indicating an amorphous state for the polymer in the membrane and denying the aggregation of the metalloporphyrin. The homogenous complexation in the membrane was also supported by a homogenous metal ion distribution in the membrane, as determined by an X-ray microanalysis. After slow and careful (such as under an inert atmosphere) solvent-evaporation, UV/vis and ESR spectroscopies on the membrane supported a homogeneous metalloporphyrin complexation having the same coordination structure even in a solid or solvent-free state over the entire membrane specimen. Accordingly, another advantage of polymer complexes is that a large amount of a gaseous molecule-carrier (metalloporphyrin) can be incorporated into the solid matrix.

1.2.4 Oxygen-Binding and Reversibility

A five-coordinate metalloporphyrin binds molecular oxygen from air selectively, rapidly, and reversibly (Eq. 1-6);

$$M(II)PL + O_2 \rightleftharpoons LPM{-}O_2 \qquad (1\text{-}6)$$

$$LPM{-}O_2 + M(II)PL \longrightarrow LPM{-}O_2{-}MPL \longrightarrow PM(III){-}O{-}M(III)P \qquad (1\text{-}7)$$

$$LPM{-}O_2 + H^+(H_2O) \longrightarrow M(III)PL + HO_2^{\bullet} \qquad (1\text{-}8)$$

$$LPM{-}O_2 \longrightarrow L + PM{-}O_2 \longrightarrow M(III)PL + O_2^{\bullet -} \qquad (1\text{-}9)$$

In Eqs. 1-6, 1-7, 1-8, and 1-9, M(II)P and M(III)P represent metalloporphyrins composed of metal(III) ions and metal(III) ions, respectively. In addition to a five-coordinate metalloporphyrin formation and its adequate oxidation potential (as mentioned above), the following requisites for reversible oxygen-binding have been elucidated to suppress the side-reactions of an oxygen adduct or irreversible oxidation of a metalloporphyrin, as represented by Eqs. 1-7 till 1-9.[10,23]

There is a strong driving force toward the irreversible formation of a stable μ-oxo-M(III)P dimer, as represented by Eq. 1-7. An oxygen-bound complex, or oxygen adduct, rapidly reacts with another deoxy M(II)PL, forming a binuclear dioxygen-bridged complex. This binuclear complex is irreversibly converted to an oxo-bridged M(III) dimer. In other words, the first problem of reversible oxygen-binding is how to inhibit dimerization.

A lot of work has been concerned with overcoming this problem, and two approaches have been successful. The first is an elegant steric approach, where a planar porphyrin is sterically substituted in a fashion that inhibits dimerization. A typical example is a picketfence metalloporphyrin or *meso*-α, α, α, α-tetrakis(*o*-

pivalamidophenyl) porphrinatometal (picketfence in Figure 1-7), which has four pivalamido groups on one side of the porphyrin plane that provide a cavity for protecting the bound oxygen from dimerization[9]. Another realistic approach attaches the metalloporphyrins to a rigid polymer chain to prevent the two metalloporphyrins from reacting with each other and dimerizing. By these means (or a combination of the first and second approach), reversible oxygen-binding to metalloporphyrins and cobalt-Schiff's base complexes has been achieved under limited conditions.

The next requisite is that the proton-driven oxidation (see Eq. 1-8) has to be retarded with a hydrophobic environment. The protein of hemoglobin embeds iron PPIX and protects it from oxidation; that is, the hydrophobic domain of the globular protein excludes water molecules and suppresses proton-driven oxidation.

Another requisite is that the oxidation induced by a ligand-off (see Eq. 1-9) has to be retarded with a stable five-coordinate complexation. Although a metalloporphyrin complex with an axial ligand (L in Eq. 1-9) is thermodynamically stable with a large K_1, as described in the previous section, the metalloporphyrin is still liable in the ligand complexation. A moment dissociation of the axial ligand in the oxygen-bound complex causes an electron transfer from the metal(II) ion to the bound oxygen molecule to yield M(III)P and a super oxide anion. A stable metalloporphyrin-polymer complexation with a large K_1 value has been characterized in comparison with monomeric complexes. For these reasons, metalloporphyrin-polymer complexes are expected to become an efficient oxygen carrier with a sufficient operational lifetime.

For example, the operational lifetime of a picketfence cobalt porphyrin-polymer complex in a solid state is much longer than that of monomeric complexes and the complex in a solution, and it maintains its oxygen-binding ability for over a month at room temperature under an air atmosphere. For a cobalt(II) porphyrin bound to a polymer ligand in a solid state, irreversible oxidation via Eq. 1-7 is inhibited because it is molecularly dispersed and immobilized on the polymer chain. The hydrophobic environment around a cobaltporphyrin excludes water vapor, thereby suppressing the proton-driven irreversible oxidation in Eq. 1-8. The static bonding of an axial ligand with a cobaltporphyrin in a solid state retards the process of Eq. 1-9. The cooperation of these effects strikingly inhibits irreversible oxidation and prolongs the lifetime of cobaltporphyrin in a solid polymer membrane. This enhanced stability of the carriers provides a great advantage for solid membranes of polymer complexes.

Oxygen-binding is monitored by a reversible change in the UV/vis absorption spectrum of an aprotic solvent solution of a metalloporphyrin-polymer complex. For example, a dichloromethane solution of a cobalt octaethylporphyrin (OEP in Figure 1-

7) complex of OIm was cooled to –15 °C.[27] The absorption of the red-colored CoOEP-OIm solution (Inset in Figure 1-9) changed from the spectrum (dark red; λ_{max} = 392 and 550 nm) ascribed to a deoxy or five-coordinate cobalt porphyrin under a nitrogen atmosphere to the spectrum (brilliant red; λ_{max} = 413, 528 and 561 nm) ascribed to an oxy cobalt porphyrin or O_2:Co = 1:1 adduct immediately after exposure to oxygen. The deoxy-oxy spectral change was reversible in response to the oxygen partial pressure with isosbestic points at 400, 519, 537, and 558nm. For a cobalt protoporphyrin IX dimethylester complex of poly(4-vinylpyridine-*co*-styrene) (PPIX, R=CH_3 and SPy in Figures 1-7 and 1-8, respectively) deoxy: λ_{max} = 404 and 555 nm, oxy: λ_{max} = 420, 543, and 575 nm, isosbestic points = 412, 548, and 565nm. Such a reversible spectral change in response to the oxygen partial pressure with isosbestic points is one of crucial evidences that a metalloporphyrin acts as an effective oxygen carrier from an equilibrium perspective. If a transparent (but red-colored) membrane could be prepared by selecting the polymer-ligand, the oxygen-binding was also confirmed and measured using visible absorption spectroscopy.

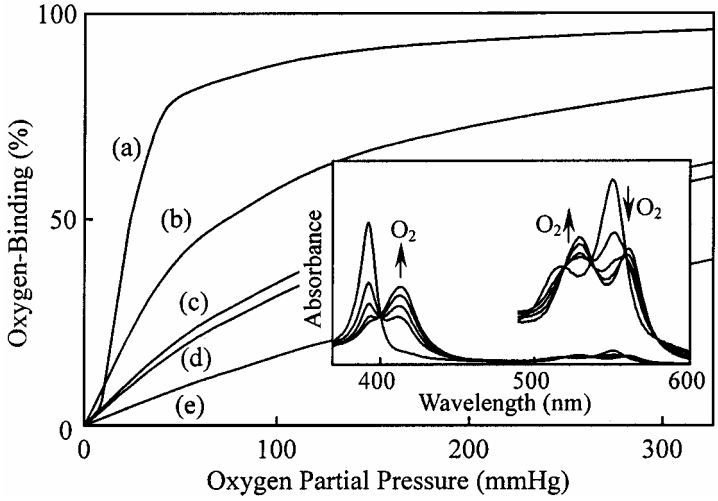

Figure 1-9. Oxygen-binding equilibrium curves for (a) cell-free hemoglobin in pH 7.4 aqueous solution at 37°C, (b) Co Picketfence-OIm in the membrane state at 25°C, (c) CoPicketfence-OIm in toluene solution at 25°C, (d) CoOEP-OIm in CH_2Cl_2 at –15°C, and (e) CoPicketfence-OPy in toluene solution at 25°C. Inset: UV-visible absorption spectral change of the CoOEP-OIm complex in CH_2Cl_2 at –15°C in response to oxygen partial pressure from 0 to 760 mmHg.

Oxygen-binding equilibrium curves were drawn from the UV/vis absorption spectral changes, as shown in Figure 1-9. The equilibrium curves obeyed Langmuir isotherms to provide the oxygen-binding equilibrium constant *K* or -binding affinity p_{50} (oxygen partial pressure at which half of the metalloporphyrins binds with oxygen), as defined by Eq. 1-10. The curves in Figure 1-9 also show that the oxygen-binding

affinity depends on both the species of metalloporphyrin and polymer-ligand and on the solution (solvent species) or solid state (and also on the temperature, as described later on). In other words, the oxygen-binding affinity can be controlled with the chemical structures of the metalloporphyrin and polymer-ligand and tuned to be adequate for the separation of oxygen from air.

$$\mathrm{LPCo} + \mathrm{O_2} \underset{k_{off}}{\overset{k_{on}}{\rightleftharpoons}} \mathrm{LPCo{-}O_2} \qquad K(=1/p_{50}) = k_{on} / k_{off} \qquad (1\text{-}10)$$

In addition to UV/vis absorption spectroscopy, oxygen-binding to a metalloporphyrin complex fixed in a solid or solvent-free membrane and film has also been confirmed in an in situ membrane state with general spectroscopies. For example, by attaching a membrane fragment to the cell window of a simple IR spectrometer, strong IR absorption at 1150 cm^{-1} for $^{16}O_2$ and 1060 cm^{-1} for $^{18}O_2$ attributed to an end-on-type coordination of molecular oxygen to the metal ion appeared with an increase in the oxygen partial pressure (Inset in Figure 1-10).[28]

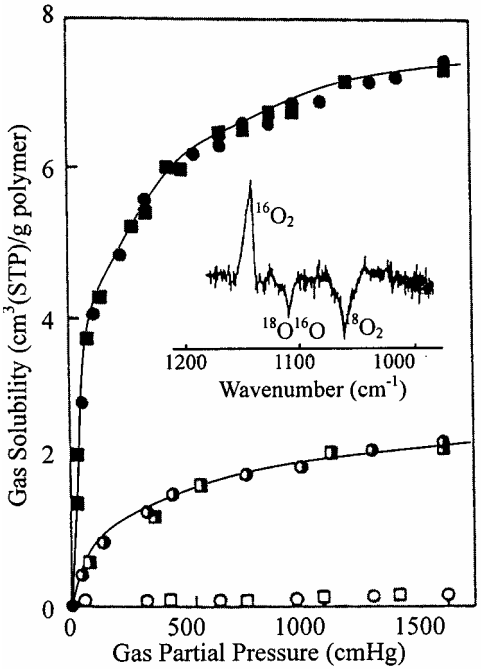

Figure 1-10. Oxygen absorption into the cobalt porphyrin-polymer membranes at 25°C. ●, ■: absorbed oxygen volume per membrane unit weight (OPy membrane containing 30 % of picketfence cobalt porphyrin), ○,□: absorbed nitrogen volume per membrane unit weight, and ◑, ◨: absorbed oxygen volume (7 wt% of cobalt porphyrin). Inset: Differential IR absorption of the Copicketfence-OIm membrane under $^{16}O_2$ and $^{18}O_2$ atmosphere.

The amount of oxygen solubility is greatly enhanced by the incorporation of a metalloporphyrin complex in a polymer, which was quantitatively measured using a microvolumetoric measurement, as described in chapter 9.2.2. (Figure 1-10).[29] For

example, the membrane of an OPy complex containing 30% picketfence cobalt porphyrin absorbed ca. 7cm^3(STP) oxygen gas/g polymer, which is more than 500 times greater than that of physically dissolved nitrogen. This extraordinarily large amount of dissolved oxygen in the polymer membrane originated from chemically specific and reversible oxygen-binding to the cobalt porphyrin complex in the polymer. As such, one of the advantages of solid polymer complexes is that a large amount of cobalt porphyrin can be incorporated into the membrane through the coordination of a nitrogenous residue of the polymer.

Figure 1-10 shows the effect of the cobaltporphyrin concentration on the oxygen solubility in the OPy sample, indicating that the amount of dissolved oxygen corresponds to the cobalt porphyrin concentration in the membrane. Figure 1-10 also reveals that the oxygen absorption behavior responds to the atmospheric oxygen pressure and is analogous to the olefin absorption in silver-polymer complexes. The oxygen absorption curves (Figure 1-10) are according to a Langmuir isotherm for the chemical dissolution to the complex and Henry's law for the physical absorption, to give K, k_D, and C_c. The curves drawn by using the dual mode sorption were in good accordance with the experimental results. The C_c value increased whereas the K value was independent of the cobaltporphyrin concentration in the sample. This data agreed with that determined spectroscopically.

It is known that metal-coordinated gaseous molecules are photodissociated under flash irradiation, and that their rapid re-binding reactions can be analyzed, based on the oxygen-binding with a metalloporphyrin (Eq. 1-11)[11,28]. The photodissociation and binding of gaseous molecules in a solid metal-polymer membrane are significantly improved with pulse and laser flash spectroscopic techniques. The oxygen-binding rate constant k_{on} and releasing rate constant k_{off} in Eq. 1-10 were estimated by second-order kinetics, and listed with the oxygen-binding (equilibrium) affinity values in Table 1-2 (see also Eq. 1-12).

$$\mathrm{LPCo{-}O_2} \xrightarrow{h\nu} \mathrm{LPCo} + \mathrm{O_2} \xrightarrow{k_{app}} \mathrm{LPCo{-}O_2} \qquad (9\text{–}11)$$

$$k_{app} = k_{on}[\mathrm{O_2}] + k_{off} \qquad (9\text{–}12)$$

Table 1-2, at first, shows that the oxygen-binding affinity of a metalloporphyrin complex can be controlled by variation of the metal species, porphyrin structure, and axial ligand species. The oxygen affinity of an iron porphyrin is around twice that of the corresponding cobalt porphyrin, while an iron porphyrin suffers irreversible oxidation due to its lower oxidation potential and its lifetime is much shorter than that of a cobalt porphyrin (a cobalt porphyrin is superior to an iron porphyrin, as an oxygen

carrier, except its toxicity in applying to medical usage). A liner relation between the affinity and the basicity of the axial ligand has been summarized for a cobalt porphyrin complexed with various nitrogenous and axial ligands:[28,33] with this relationship one can explain the affinity of OIm > OPy in Table 1-2. It can be also noted in Table 1-2 that such higher oxygen affinities (smaller p_{50} or larger K in Eq. 1-10) are caused by smaller oxygen-releasing rate constants (k_{off}, that is, $K = k_{on} / k_{off}$).

Table 1-2. Oxygen–binding affinity (p_{50}) and binding rate constants (k_{on} and k_{off}) for the metalloporphyrin–polymer complexes at 25°C.

Metallo-porphyrin	Axial ligand	State	p_{50} cmHg	10^{-5} k_{on} M^{-1} s^{-1}	10^{-4} k_{off} s^{-1}	Ref.
Hemoglobin[a]	–	soln	1.4	170[b]	0.0013[b]	30
CoPicketfence	OIm	soln[c]	25	84	73	4,29
CoPicketfence	OIm	membr	7.6	1.7	1.2	11,26
CoPicketfence	OPy	membr	16	1.9	2.6	31
FePicketfence	OIm	membr	3.2	0.47	0.13	32

[a] Cell-free-hemoglobin in pH 7.4 aqueous solution,[b] 37°C.

1.3 Small Molecule Transport Through Membranes of Metal Complexes in Macromolecules

1.3.1 Membrane Gas Separation

Membrane separation of gaseous small molecules through the dense (non-porous) polymeric membranes occurs because of differences in solubility and diffusivity, while membrane performance is characterized by permeability and selectivity. The permeability of component *i*, P_i, is defined as the product of the diffusion and solubility coefficients (D_i, and S_i, respectively) (Eq. 1-13).

$$P_i = D_i S_i \qquad (1\text{-}13)$$

The selective property of a membrane towards a mixture is generally expressed by the ideal separation factor or selectivity. The ideal separation factor α_{ij} is defined as the ratio of two pure gaseous molecule permeabilities (Eq. 1-14).

$$\alpha_{ij} = P_i / P_j \qquad (1\text{-}14)$$

In membrane separation processes for two components, the feed stream is a mixture, as such, the ideal separation factor is often unsuitable for describing the real separation performance. Therefore, the selectivity A_{ij} is defined differently, where x_i and y_i are the concentrations of component *i* for the feed and permeate streams,

respectively (Eq. 1-15).

$$A_{ij} = (y_i/y_j)/(x_i/x_j) \quad (1\text{-}15)$$

A_{ij} depends on the membrane material properties and the experimental conditions, whereas α_{ij} only depends on the membrane material properties. Thus, the permeability and ideal separation factor are mostly used to characterize the transport properties of membrane materials. Note that A_{ij} is converted to α_{ij} when the permeate side is held in a vacuum for pure gas experiments.

A composite membrane, comprising a thin (ca. 1 μm) top layer of metal-polymer complexes on an asymmetric porous support, is mostly used for practical applications to provide a high separation performance and mechanical strength. Membrane separation usually occurs on the top dense layer of metal-polymer complexes, while the asymmetric porous support provides mechanical strength. Accordingly, the thickness of the top layer is important in determining the separation properties and should be measured precisely. However, since a precise measurement of the top layer is open extremely difficult, the permeability is hard to measure. Consequently, the thickness normalized permeability, called the permeance Q_i hereafter, is frequently used and defined as $Q_i = P_i/L$, where L is the effective top layer thickness of the membrane. The permeance Q_i depends on the membrane material properties as well as the membrane structure. As a result, the permeation property of a membrane can be characterized by either its permeability or permeance.

To achieve a high separation performance, the permeability and selectivity should both be high. However, a trade-off behavior between the permeability and selectivity is commonly observed in polymeric membranes:[34] the permeability is high when the selectivity is low, and visa versa. One effective way to overcome such trade-off behavior is to employ the concept of *facilitated transport*.[35] In facilitated transport membranes, carriers are incorporated into the membrane. The carrier is any compound, often transition metal ions or complexes, that binds *reversibly* with a specific gaseous molecule. The reversible binding for a specific gaseous molecule induces additional mass transport, referred to as "carrier-mediated" transport. Thus, the total mass transport is the summation of the carrier-mediated transport and Fickian transport, facilitating the permeation of the specific gaseous molecule, thereby resulting in a high permeability and high selectivity. The characteristics of facilitated or carrier-mediated transport result from the occurrence of a reversible binding reaction in combination with a Fickian diffusion process. The choice of the carrier (or metal complex) is a key factor in facilitated transport. For example, a high selectivity is obtained if the carrier's binding reaction is reversible and kinetically active to a particular small molecule and

the rates of the binding and releasing reactions of the small molecule with the carrier are very high.

In facilitated transport membranes, the carriers can be dissolved in a liquid solvent or fixed to a solid polymer matrix. When the carriers are dissolved in a liquid medium, the carriers at the upstream interface react with a specific small molecule to form an adduct, which then moves across the membrane and releases the small molecule from the adduct due to a releasing reaction, as shown in Figure 1-11a. As such, the separation property depends on the binding and releasing reaction rates as well as the mobility of the adduct in the liquid medium.

A liquid-free, solid-state membrane containing fixed carriers can also provide high permeability as well as high selectivity. Figure 1-11b schematically represents facilitated transport membranes with fixed carriers. The fixed carriers at the upstream interface bind with a specific small molecule to form an adduct. The small molecules bound to the carrier is then released in the matrix or transferred to other carriers in response to a concentration gradient. The binding and releasing reactions occur repeatedly across the membrane. At the membrane-downstream interface, the carrier adduct releases the small molecule to the downstream side, thereby resulting in facilitated transport. Thus, the small molecule's solubility, and binding-releasing reaction rates between the carrier (the metal complex) and the small molecule are major parameters in determining the transport properties. Fixed carrier membranes in a solid state provide the following advantages over liquid membranes: (1) higher stability of the carrier, (2) higher mechanical strength, (3) no liquid loss, (4) possibility of incorporating a larger amount of the carrier in the matrix, and (5) flexibility as regards controlling the membrane thickness to enhance the flux.

Since the transport of a small molecule through a fixed carrier membrane depends largely on the kinetics, reversibility and affinity of the small molecule to the metal complex carrier, the transport properties of a small molecule are a good index for the activity of a metal complex in a macromolecule. Therefore, the following sections give a brief review of facilitated olefin and oxygen transport.

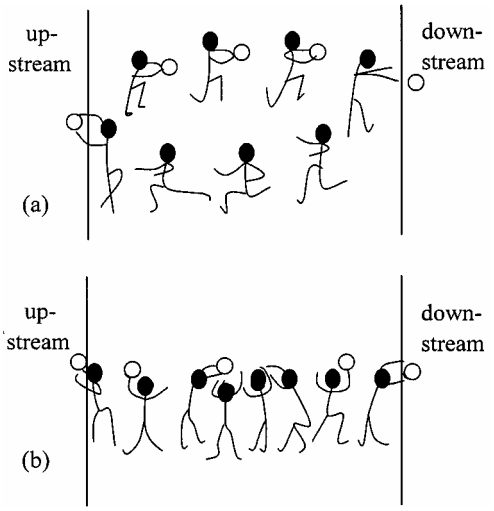

Figure 1-11. Facilitated transport in (a) liquid, and (b) solid state.

1.3.2 Facilitated Olefin Transport

The separation of olefin/paraffin gas mixtures is one of the most energy intensive processes in petrochemical industries, because it is mainly performed by cryogenic distillations. Membrane processes using the concept of facilitated transport have been considered as an intriguing alternative to cryogenic distillation, as they can simultaneously improve the permeability and selectivity. Silver ions incorporated in liquid membranes act as olefin carriers for facilitated olefin transport, resulting in a high separation performance for propylene/propane or ethylene/ethane mixtures. However, such liquid membranes suffer from the disadvantage that liquid water must be added to the feed stream to activate the silver salt (solvate the silver ions) and then removed from the permeate stream.[36-39] Therefore, a facilitated transport membrane in a solid state is more desirable.

To make facilitated transport membranes in a solid state, silver salts, such as $AgBF_4$, are complexed with polar polymers, PEO,[40] POZ, and PVP,[13] as described in the Experimental example 9.5.2. Figure 1-12 shows the propylene permeance through $AgBF_4$-POZ and $AgBF_4$-PVP membranes with an increasing amount of silver and constant feed pressure at 414 kPa.[12] The propylene permeance through the membranes shows a similar trend with an increasing silver salt content, and no significant increase in the propylene permeance is observed until the mole ratio of silver to carbonyl reaches above 0.33, from which point the propylene permeance increases almost linearly with the silver concentration up to 3.0 $x10^{-5}$ $cm^3(STP)/cm^2sec$ cmHg. This linear increase in the propylene permeance is consistent with theoretical predictions

based on the concentration fluctuation theory, as described in 9.3.3. While no significant dependence of either polymer matrix is evident under these experimental conditions, the anions of the silver salt have a significant effect on the facilitated transport.

The mole ratio of silver ions to carbonyl oxygen is fixed at 1 in the silver-POZ (or -PVP) complexes, that is, $[Ag^+]:[C=O] = 1:1$ (ca. 80 wt% of $AgBF_4$). The permeance of pure propylene through the membranes is then plotted as a function of the feed pressure, as shown in the inset in Figure 1-12. The polymer membranes containing $AgBF_4$ in POZ or PVP exhibited a propylene permeance of 4.5 $x10^{-5}$ $cm^3(STP)/cm^2sec$ cmHg at 140 kPa, whereas the propylene permeance through the pure POZ or PVP membrane was only ca. 5.0 x 10^{-8} $cm^3(STP)/cm^2sec$ cmHg. As such, the propylene permeance with the silver-polymer complex membranes is more than three orders of

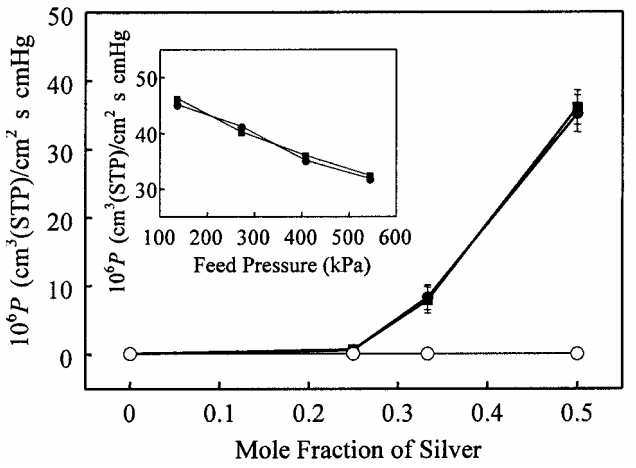

Figure 1-12. Propylene permeance and propylene/propane selectivity with increasing carrier concentration.[12] ●: $AgBF_4$/POZ, ■: $AgBF_4$/PVP and ○: propane.

magnitude higher than that with the pure POZ or PVP, clearly demonstrating the facilitated transport of propylene due to the presence of silver ions. Conversely, the propane permeance decreased from 5.0 $x10^{-8}$ to 3.0 x 10^{-9} $cm^3(STP)/cm^2sec$ cmHg with the silver concentration. Thus, the ideal separation factor of propylene over propane is approximately 15,000. As a result, a propylene concentration higher than 98 % is observed in the downstream side after only a single pass of the silver-polymer complex membranes when 50 % propylene is used as the feed stream. For further details, refer to Experimental example 9.5.2.

Rubbery polyether-based polymer membranes containing silver ions also exhibit a good separation performance for an olefin/paraffin mixture gas. The pure gas permeation through membranes consisting of PEO and $AgBF_4$ is presented in Table 1-

3[40]. The ethylene/ethane and propylene/propane selectivities of the pure PEO membrane were only 1.2 and 2.5, respectively. The PEO membrane containing 33wt% $AgBF_4$ ($[Ag^+]$:[-O-] = 1:8) also had poor separation properties. However, when the silver concentration reached [Ag]:[-O-] = 1:1, the pure ethylene and propylene permeances are 50−100 times higher than those of the pure PEO membrane. As such, these results have direct implications for facilitated olefin transport in solid-state polymer membranes.

1.3.3 Facilitated Oxygen transport

The facilitated transport of molecular oxygen through a solid polymer complex membrane was first achieved by incorporating a picketfence cobalt porphyrin, characterized with both rapid kinetics and a strong affinity for oxygen-binding, as a chemically selective oxygen-binding site.[5,11] The oxygen permeability coefficient P_{O2} for the membrane is shown in Figure 1-14.[5,41] P_{O2} is larger than P_{N2} and steeply increases with a decrease in the oxygen upstream pressure (p_{O2}). Conversely, P_{N2} is small and independent of the nitrogen upstream pressure (p_{N2}), because the fixed cobalt porphyrin does not interact with nitrogen. P_{O2} is also small and independent of p_{O2} for the control membrane composed of an inert Co(III) complex, which does not interact with oxygen. As such, the active cobalt porphyrin fixed in the polymer membrane facilitates oxygen transport and enhances the oxygen permeation, represented by the shadowed area in Figure 1-14. P_{O2} also increases with the cobalt porphyrin concentration in the polymer membrane. The oxygen/nitrogen selectivity was 3.2, 4.4, and 7.5 for a membrane containing 0, 2.5, and 4.5 wt% picketfence cobalt porphyrin, respectively. These results indicate a high selectivity and high permeability for a solid-state polymer membrane containing an oxygen carrier.

The time course of the permeation of gaseous molecules through the membranes exhibited an induction period followed by permeation with a constant slope (steady state). The induction period (θ) for oxygen permeation was longer than θ for nitrogen and was also prolonged with a decrease in p_{O2} (Inset in Figure 1-14).[41] In contrast, θ for nitrogen permeation was short and independent of p_{N2}. This behavior indicates that oxygen clearly interacts with the cobalt porphyrin in the polymer membrane and that its diffusivity in the membrane is reduced by repeated oxygen binding and release on the fixed cobalt porphyrin. θ_{O2} was prolonged depending on the cobalt porphyrin concentration in the membrane.

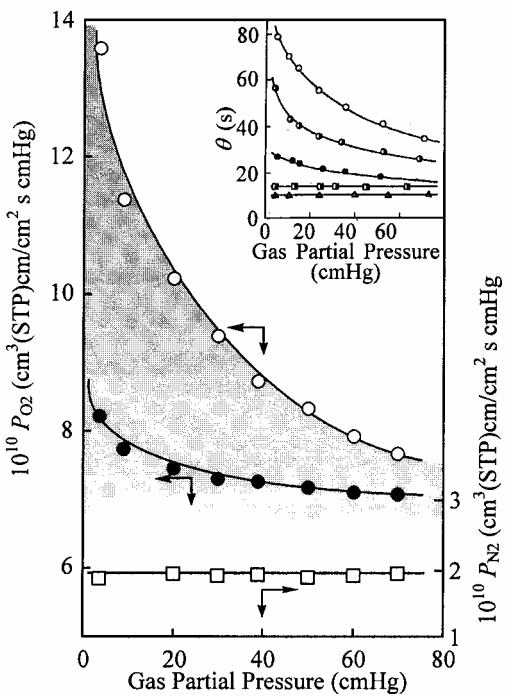

Figure 1-14. Oxygen and nitrogen permeability coefficients (P_{O2} and P_{N2}) for the cobalt porphyrin-polymer complex membrane. The cobalt porphyrin concentration in the OIm membrane: ○: 4.5 %; ●: 2.5 %; and □: nitrogen for 4.5 % at 30 C. Inset: Effect of gas partial pressure on induction period (θ) for the permeation through the membrane of 4.5 % cobalt porphyrin. oxygen at ○: 20°C; ◑: 25°C, and ●: 30°C; ◨ nitrogen at : 25°C; and oxygen at ◭: 25°C for the inert cobalt(III) porphyrin membrane.

θ_{O2} and the p_{O2}-dependency of θ_{O2} were enhanced at lower temperatures, because the oxygen-binding rate constants decreased and the oxygen affinity K increased with a decreasing temperature. As such, θ is the best parameter to distinguish whether or not the metal complex fixed in the polymer membrane contributes to the transport of a gaseous molecule through the membrane.

Scheme (Figure 1-11b) represents the facilitated transport of oxygen via a fixed carrier (cobalt porphyrin) in a solid membrane. The fixed carrier picks up oxygen specifically from air at the upstream interface. This specific and reversible oxygen-binding reaction establishes a steep gradient in the oxygen concentration across the membrane from the upstream side to the downstream side, in response to which the oxygen taken up in the membrane is transferred via the fixed carriers to the downstream side (if the passage of the oxygen by the fixed carrier is efficient and rapid). That is, the driving force to yield the facilitated oxygen transport is the concentration gradient of oxygen in the membrane or selectively enhanced solubility

of oxygen, as demonstrated, for example, by the results in Figure 1-10.

The above results and consideration suggest that a dual-mode-transport model, derived from the dual-mode-absorption model (Eq. 1-4), is applicable to analyze the oxygen transport in cobalt porphyrin-polymer membranes. Figure 1-15 is a schematic representation of the oxygen permeability in a cobalt porphyrin-polymer membrane governed by two modes.[11] That is, the oxygen permeation is equal to the sum of the first term that represents the physical permeation mode and the second term that represents the carrier-mediated mode. For the physical mode (upper permeation route in Figure 1-15), oxygen physically dissolves in the polymer membrane according to Henry's law, then the dissolved oxygen diffuses physically. For the carrier-mediated mode (the lower permeation route in Figure 1-15), oxygen is specifically and chemically taken up by the cobalt porphyrin fixed in the membrane and hops from one cobalt porphyrin to another by repeating a binding and releasing reaction to and from the cobalt porphyrin. The oxygen transport is thus accelerated by this carrier-mediated mode in addition to the physical mode.

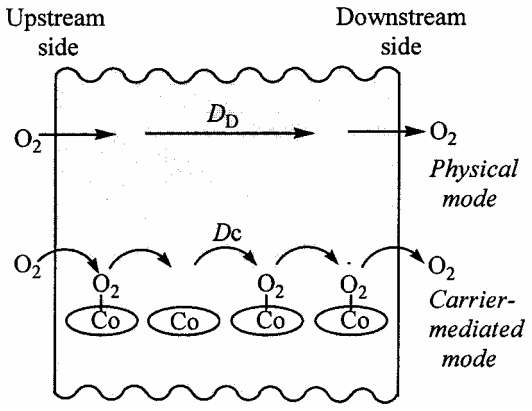

Figure 1-15. Dual-mode oxygen transport in the solid-state polymer membrane containing cobalt porphyrin as a fixed carrier of oxygen

The dual-mode-transport model is mathematically described in Eq. 16.

$$P_{O2} = k_D D_D + \frac{D_c C_c K}{1 + K p_{O2}} \qquad (1\text{-}16)$$

Here, D_D is the physical diffusion coefficient of oxygen in the membrane, and D_C is the postulated diffusion coefficient of oxygen that hops via the fixed cobalt porphyrin carriers. k_D and C_C are measured by an absorption experiment (for example, Figure 1-10). C_C corresponds to the concentration of active cobalt porphyrin incorporated in the membrane and K is the oxygen-binding equilibrium constant of the

cobalt porphyrin fixed in the membrane, which is spectroscopically measured (for example, as given in Table 1-2).

The effect of p_{O2} on P_{O2} in Figure 1-15 was analyzed using Eq. 1-16, that is, P_{O2} was plotted versus $1(1 + Kp_{O2})$.[5,41] The plots showed a linear relationship to yield the diffusion coefficients, $D_D = 10^{-6}$ cm^2 s^{-1} and $D_C = 10^{-8}$ cm^2 s^{-1}. The D_D value agreed with the previously reported diffusion coefficient of oxygen in an amorphous polymer with a similar T_g. D_C, representing the oxygen diffusion via the fixed cobalt porphyrin carriers, is smaller than D_D, because the chemical binding reaction of oxygen with the cobalt porphyrin suppresses the oxygen diffusivity. D_C increased with C_C or the active cobalt porphyrin concentration in the membrane. D_C has been found to be inversely proportional to the average distance between the cobalt porphyrin sites,[42] thereby supporting the postulation that D_C represents the oxygen diffusivity hopping via the fixed cobalt porphyrin carriers, as illustrated in Figure. 1-15. An increase in the cobalt porphyrin concentration in the membrane, that is, C_C, resulted in an apparent increase in D_C. The multiplication of the increases in both C_C and D_C significantly enhances the second (chemical) term in Eq. 1-16. As a result, both P_{O2} and the oxygen/nitrogen permselectivity increase with the active cobalt porphyrin concentration in the membranes, which can be clearly ascribed to the cobalt porphyrin-mediated transport or facilitated oxygen transport by the fixed cobalt porphyrin carriers.

1.3.4 Other Small Molecule Transport

Small molecular transport other than olefin and molecular oxygen facilitated transport through a metal-polymer complex containing carriers (silver ions and metalloporphyrins, respectively) has also received attention, such as nitrogen transport by a cyclopentadienylmanganese and benzenechromium complex attached to a polymer,[44,45] and CO_2 and H_2S transport based on ion exchange membranes containing a diamine complexing agent.[46,47] The facilitated transport of SO_2 through supported liquid membranes has also been observed in membranes containing water, aqueous neutral salt solutions, and aqueous sodium hydroxide solutions as the carrier.[48]

1.4 Other Applications of Metal Complexes in Macromolecules with Small Molecule-Binding Abilities

The main application of the specific and reversible binding ability of small molecules to metal complexes in macromolecules is in gas separation membranes. Another application of the binding between gaseous small molecules and a metal-polymer complex is as an absorbent. The powder of silver-polymer complexes absorbs

olefin selectively under atmospheric pressure (or at ambient temperature) by the formation of an adduct, then releases the absorbed gas under reduced pressure (or at a high temperature) using a pressure (or thermal) swing method. Since most metal complexes are easily deactivated by a reaction with other components, especially with water, in a gas mixture, the polymers in metal-polymer complexes play an important role in protecting and supporting the metal complexes. When silver-polymer complexes were prepared from a mixture of polystyrene and 23.2 mmol of silver chloride and aluminium chloride in the matrix, the absorption of ethylene (contained in water) under 1 atm at room temperature by the silver-polymer complex was very rapid. The equilibrium molar ratio of absorbed ethylene to the admitted silver ion was 1.01 after 2 hrs. The solid polymer complex repeatedly exhibited an absorption of ethylene without any apparent deterioration, even in the presence of water.

Copper-polymer complexes also retain an important position as regards binding with ethylene. When a solid polymer complex was prepared from polystyrene beads, copper(I) chloride, and aluminum chloride, the absorption at room temperature by the polymer complex was rapid, and the equilibrium molar ratio of absorbed ethylene to the admitted copper (I) chloride was 1.40. The amount of ethylene absorbed by 1 g of the polymer complex solid was 89 cm^3(STP).

A porous polymer complex[26] containing 30 % picketfence cobalt porphyrin absorbed ca. 4 cm^3(STP) of oxygen per gram of polymer, which is more than 500 times that of physically dissolved nitrogen, and provided oxygen-enriched (oxygen concentration in the product flow: 45 %) air when using a pressure swing method. In addition, polymer complexes with a cobalt Schiff base (Co-salen in Figure 1-7) have been tested as a sensor and oxygen absorbent.[49]

Several optical sensors have already been introduced that selectively respond to oxygen in the atmosphere or water. A calorimetric oxygen sensor has been tested using a solid polymer membrane or coating involving a picketfence cobalt porphyrin. The polymer cobalt porphyrin membranes are characterized by a deep red color, and the oxygen-adduct formation is accompanied by a color change or sharp deoxy-oxy spectral change with the isosbestic points (for example, see inset in Figure 1-9). When the oxygen response was monitored at the oxy absorption maximum at 547nm, the 90 % response time for a 20μm-thick fluorinated OIm-picketfence cobalt porphyrin membrane was 5s and the operational lifetime was longer than 3 months.[50] Membranes of picketfence cobalt porphyrins complexed with three kinds of polymer-ligands, OPy, OIm, and O4Im, were characterized by a different oxygen affinity, which increased by a factor of 10. The three cobalt porphyrin complex membranes

displayed a selective and continuous response over a very wide range of oxygen partial pressures from 0.01 to 76 cm Hg.[31]

The most frequently used optical oxygen sensors are related to the luminescence quenching of organic dyes by molecular oxygen. A novel oxygen sensing coating has been reported based on a combination of the luminescence quenching by oxygen and oxygen-binding of cobalt porphyrins.[51] As illustrated in Figure 1-17, the body surface of a model is first coated with a polymer layer containing luminescence dye molecules, such as pyrene. The emission from the dye molecules is then decreased by quenching with oxygen which obeys Stern-Volmer equation. The dye molecule layer is further coated with a polymer-picketfence cobalt porphyrin layer. The UV/vis absorption of the cobalt porphyrin is red-shifted in response to the oxygen-adduct formation or oxygen pressure, which overlaps and reduces the emission from the dye molecules. The sum of the two emissions decreases along with an increase in the oxygen pressure, yielding a non-Stern-Volmer type response or high sensitivity to the oxygen pressure. This polymer cobalt porphyrin coating is currently being tested as an oxygen pressure (that is, atmospheric total pressure)-sensitive paint for unsteady wind-tunnel experiments related to aircraft and automobile development.

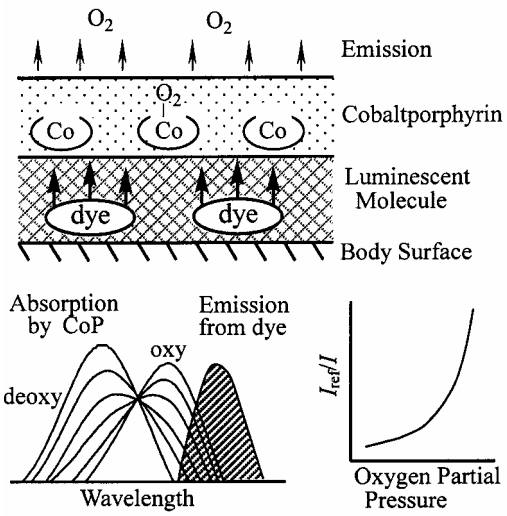

Figure 1-17. A novel oxygen-sensing coating based on combination of a luminescent dye molecule and an oxygen-binding cobalt porphyrin. Lower left: Overlapping of absorption by the cobalt porphyrin with emission from the dye molecule. Lower right: Stern-Volmer plots (I_{ref}/I: normalized luminescence intensity).

The reversible oxygen-binding property of a picketfence cobalt porphyrin allows the efficient accumulation of oxygen from an aqueous solution, which contributes to an increase in the diffusion-limited current for the electroreduction of oxygen, as

illustrated in Figure 1-18.[52] When a cobalt porphyrin-OIm complex is coated on a glassy carbon surface, the advantages of the polymer complex include nonvolatility, insolubility in the aqueous phase, and a long operational lifetime for the cobalt porphyrin. The reduction current of oxygen for the cobalt porphyrin membrane was significantly larger than that for the control membrane without any cobalt porphyrins and remarkably increased with the cobalt porphyrin concentration. For example, the reduction current of oxygen for a 50 mM cobalt porphyrin membrane was around 10 times higher than that for the control membrane (Figure 1-18). The reduction current obeyed a Langmuir type model, while that of the control membrane followed a Henry type model. The results of rotating platinum ring-glassy carbon disk voltammetry suggested that over 90 % of the oxygen was reduced by four electrons to hydroxyl, regardless of the basicity of the aqueous solution. These results demonstrate that the cobalt porphyrin complex accumulates oxygen from the aqueous phase, then supplies it to the electrode surface, which could be practically applied to air-assisted batteries and fuel cells.

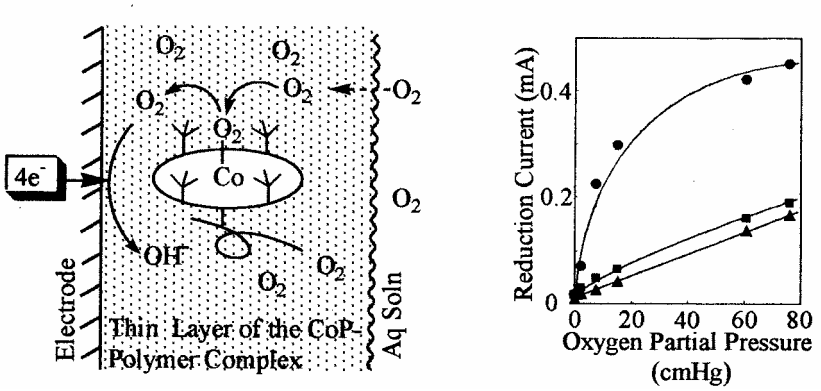

Figure 1-18. Electroreduction of oxygen accumulated in the cobalt porphyrin membrane at an electrode (Scheme). Reduction current of oxygen for the electrode modified with ●: 50 mM, ■: 5 mM cobalt porphyrin, and ▲: without cobalt porphyrin.

In a solution, the oxygen-binding ability of a variety of cobalt(II) ion complexes has also been studied . An important class of such complexes is represented by cobalt(II) amine complexes in an aqueous solution. Their oxygen adducts have been characterized as μ-peroxo cobalt(III) complexes (or $[O_2]$:[Co] = 1:2 type or sandwiched type), as shown in Eq. 1-18, using the example of a cobalt-hexamine complex.

$$2Co(II)(NH_3)_6 + O_2 \rightleftharpoons (NH_3)_5Co(III)\text{-}O_2^{2-}\text{-}Co(III)(NH_3)_5 + 2NH_3 \quad (1\text{-}18)$$

Oxygen adducts are readily formed by the air bubbling of a cobalt amine complex solution. Similar μ-peroxo cobalt(III) complexes are formed by the reaction of oxygen with a variety of cobalt(II) chelates. The amine ligands in oxygen-binding complexes also have been extended to polyamines, such as poly(ethyleneimine). (details are given in Experimental chapter 9.5.4)

In the blood stream of mammals, serum albumin (molecular weight 66500 Da) is the major plasma protein and plays two main roles: maintaining the colloid osmotic pressure, and transporting many helpful materials around the body. Employing these fundamental functions, serum albumin has been used as a plasma expander and therapeutic drug carrier in the circulatory system. From the viewpoint of clinical application, providing serum albumin with an oxygen-carrying capability is of significant interest[53]. Accordingly, an iron TPP derivative with a covalently linked imidazole ligand, for example, 2-[8-{N-(2-methylimidazolyl)}octanoyloxymethyl]-5,10,15,20-tetrakis(α,α,α,α-*o*-pivaloylamino)phenylporphinatoiron, has been synthesized, then, a small amount of its ethanol solution was incubated with an aqueous solution of recombinant human serum albumin. As a result, the iron porphyrin is included in the albumin and the colorless albumin solution becomes a deep red color. The iron porphyrin included in the albumin and solubilized in the aqueous solution can bind and release oxygen reversibly under physiological conditions (in aqueous media, pH 7.3, 37^{o}C), like hemoglobin and myoglobin. When a maximal eight ironporphyrin molecules are incorporated into the albumin host (Figure 1-19), the oxygen transport amount is superior to that of hemoglobin (4 iron porphyrins involved in the protein with a molecular weight of 64500 Da, see chapter 2). Spectroscopies supporting the iron porphyrin incorporation do not reveal any changes in the albumin's higher structures, plus the iron porphyrins are surrounded by a hydrophobic environment. The iron porphyrin-albumin solution exhibits a good compatibility with whole blood. Consequently, this entirely synthetic iron porphyrin-recombinant albumin is currently being studied as a new type of blood substitute[30].

Selective and reversible binding of small molecules to the metal complexes in macromolecules is now providing potential applications of metal-polymer complexes as gas transporting materials, gas separation membranes, and gas sensors. This chapter indicated that the small molecule-binding kinetics and equilibria are strongly affected by the surrounding macromolecular environment and that the metal-polymer complexes as a material display a performance different from that of the simple mixture of a transition metal ion or complex with a polymer.

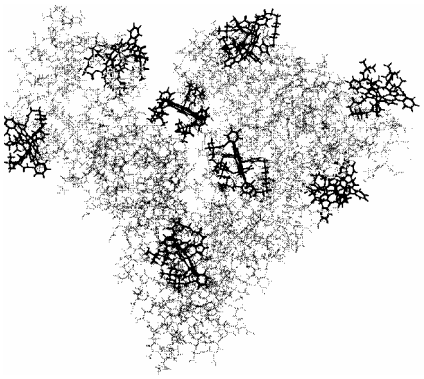

Figure 1-19. Three dimensional structure of the serum albumin including iron porphyrins as an oxygen-carrying blood substitute.

The small molecule-binding to a metal ion is the simplest and most elementary reaction; for example, the first step of the catalytic actions described in the following chapters 11 and 12. The features of metal-polymer complexes described by the binding properties of small molecules are also appropriate for these properties. While this chapter focused on the metal-polymer complexes having a homogeneous structure, crucial advantages of metal-polymer complexes are quite variable depending on the selection of the metal ion and polymer species and tailor-made structural variety. Expected examples are an alignment of metal moieties along a polymer matrix, a sequential array of different metal complexes, an interfacial assembly of metal complexes upon a nanometer-sized asymmetric membrane, and so on. They could yield unique binding performances such as an integrated small molecule-binding process, a cascade-like flux of gaseous molecules, and the formation of a gaseous molecule transport channel. The metal-polymer complexes with such designed structures may open new systems for the super efficient utilization of gaseous small molecules.

References

1. A. E. Martell, M. Calvin, *Chemistry of the Metal Chelate Compounds*, Prentice-Hall, New York, 1952.
2. R.D. Jones, D.A. Summerville, F. Basolo, *Chem. Rev.*, **79**, 139 (1979).
3. J.E. Huheey, *Inorganic Chemistry: Principles of Structure and Reactivity*, Harper International Si Edition, Cambridge, 1983**.**

4. E. Tsuchida, H. Nishide, *Adv. Polymer Sci.*, **24**, 1 (1997**)**.
5. H. Nishide, E. Tsuchida, *Macromolecule Metal Complexes*: F. Ciardelli, E. Tsuchida, D. Wöhrle (Eds.) Springer-Verlag, Berlin, 1996.
6. F.R. Hartley, *Chem. Rev.*, **73**, 163 (1973).
7. C.D. Beverwijk, G.J.M. van der Kerk, A.J. Leusink, J.G. Noltes, *Organomet. Chem. Rev. A.*, **5**, 215 (1970).
8. D.J. Safarik, R.B. Eldridge, *Ind. Eng. Chem. Res.*, **37**, 2571 (1998**)**.
9. J.P. Collman, *Acc. Chem. Res.*, **10**, 265 (1977).
10. E. Tsuchida, H. Nishide, *Topics Curr. Chem.***, 132**, 64 (1986).
11. H. Nishide, E. Tsuchida, *Polymer for Gas Separation*: N. Toshima (Ed.) VCH Publishers, New York, Chapter 6, 1992**.**
12. Y. Yoon, J. Won, Y. S. Kang, *Macromolecules*, **33**, 3185 (2000).
13. S.U. Hong, T.H. Jin, J. Won, Y.S. Kang, *Adv. Mater.*, **12**, 968 (2000).
14. S. Choi, J.H. Kim, Y.S. Kang, *Macromolecules*, **34**, 9087 (2001).
15. S.U. Hong, C.K. Kim, Y.S. Kang, *Macromolecules*, **33**, 7918 (2000).
16. S.U. Hong, J.Y. Kim, Y.S. Kang, *Polym. Adv. Technol.*, **12**, 177 (2001).
17. S. Sunderrajan, B.D. Freeman, C.K. Hall, *Ind. Eng. Chem. Res.*, **38**, 4051 (1999).
18. C.K. Kim, H.S. Kim, J. Won, Y.S. Kang, C.K. Kim, C.K. Kim, *J. Phys. Chem. A.*, **105**, 9024 (2001).
19. C.K. Kim, J. Won, H.S. Kim, Y.S. Kang, H.G. Li, C.K. Kim, *J. Comput. Chem.*, **22**, 827 (2001).
20. J.H. Jin, S.U. Hong, J. Won, Y.S. Kang, *Macromolecules*, **33**, 4932 (2000).
21. H.S. Kim, J.H. Ryu, H. Kim, B.S. Ahn, Y.S. Kang, *Chem. Commun.*, 1261 (2000).
22. J.H. Ryu, H. Lee, Y.J. Kim, Y.S. Kang, H.S. Kim, *Chem. Eur. J.*, **7**, 1525 (2001).
23. M. Momenteau, C.A. Reed, *Chem. Review.*, **94**, 659 (1994).
24. K.M. Kadish, K.M. Smith, R. Guilard (Ed.), *The Porphyrin Handbook*, Academic Press, Oxford, 1996**,** Vol. 4**.**
25. D. Dolphin (Ed.), *The Porphyrins*, Vol. V, Academic Press, New York, 1978.
26. H. Nishide, X.S. Chen, E. Tsuchida, *Functional Monomers and Polymer*: K. Takemoto, R.M. Ottenbrite, M. Kamachi (Eds.), Marcel Dekker, NewYork, 1997, Chapter 6.
27. H. Shinohara, T. Arai, H. Nishide, *Macromol. Symp.*, **186**, 135 (2002).
28. H. Nishide, E. Tsuchida, *Macromolecular Complexes*: E. Tsuchida (Ed.) VCH Publishers, New York, 1991, Chapter 6.
29. H. Nishide, H. Kawakami, S. Toda, E. Tsuchida, Y. Kamiya, *Macromolecules*, **24**, 5851 (1991).

30. E. Tsuchida (Ed.), *Blood Substitutes*, Elsevier, Amsterdam, 1998**.**
31. Y. Suzuki, H. Nishide, E. Tsuchida, *Macromolecules*, **33**, 2530 (2000).
32. M. Ohyanagi, H. Nishide, K. Suenaga, E. Tsuchida, *Macromolecules*, **21**, 1590 (1988).
33. E Tsuchida, H. Nishide, M. Ohyanagi, O. Okada, *J. Phys. Chem.*, **92**, 6461 (1988).
34. L. M. Robeson, *J. Membr. Sci.*, **62**, 165 (1991).
35. M. Mulder, Basic Principles of Membrane Technology, 2nd Ed. In: Kluwer Academic Publishers, (1996).
36. J.S. Yang, G.H. Hsiue, *J. Membr. Sci.*, **138**, 203 (1998).
37. W.S. Ho, D.C. Dalrymple, *J. Membr. Sci.*, **91**, 13 (1994).
38. T. Yamaguchi, C. Baertsch, C.A. Koval, R.D. Noble, C.N. Bowman, *J. Membr. Sci.*, **117**, 151 (1996).
39. S. Bai, S. Sridhar, A. A. Khan, *J. Membr. Sci.*, **147**, 131 (1998).
40. (a) I. Pinnau, L.G. Toy, C. Casillas, *U. S. Patent*, 5670051 (1997); (b) I. Pinnau, L.G. Toy, *J. Membr. Sci.*, **184**, 39 (2001).
41. H. Nishide, M. Ohyanagi, O. Okada, E. Tsuchida, *Macromolecules*, **20**, 417 (1987).
42. H. Nishide, H. Kawakami, T. Suzuki, Y. Azechi, Y. Soejima, E. Tsuchida, *Macromolecules*, **24**, 6306 (1991).
43. H. Nishide, T. Suzuki, H. Kawakami, E. Tsuchida, *J. Phys. Chem.*, **98**, 5084 (1994).
44. H. Nishide, H. Kawakami, Y. Kurimura, E. Tsuchida, *J. Am. Chem. Soc.*, **111**, 7175 (1989).
45. Y. Kurimura, F. Ohta, J. Gohta, H. Nishide, E. Tsuchida, *Macromol. Chem.*, **183**, 2889 (1982).
46. R. Quinn, D.V. Laciak, *J. Membr. Sci.*, **131**, 49 (1997).
47. J.J. Pellegrino, M. Ko, R. Nassimbene, M. Einert, *Gas Separation Technology*, E.F. Vansant, R. Dewolfs (Eds.), Process Technology Proceedings, 8, Elsevier, Amsterdam (1990)**.**
48. M. Teramoto, Q. Huang, T. Maki, H. Matsuyama, *Separation and Purification Technology*, **16**, 109 (1999).
49. D. Wöhrle, H. Bohlen, *Makromol. Chem.*, **187**, 2081 (1986).
50. S. Röösli, E. Pretsch, W.E. Morf, E. Tsuchida, H. Nishide, *Analytica Chimica Acta*, **338**, 119 (1997).

51. K. Asai, Y. Egami, T. Sakai. H. Nishide, *J. Thermophys. Heat Trans*., **16**, 109 (2002).
52. B. Shentu, K. Oyaizu, H. Nishide, *Chem. Lett*., **7**, 12 (2002).
53. E. Tsuchida, T. Komatsu, K. Hamamatsu, Y. Matsukawa, J. Wu, *Bioconjugate Chem*., **10**, 797 (1999).
54. K. Oyaizu, H. Nakano, B. Shentu, H. Nishide, *J. Mater. Chem.*, **12**, 3162 (2002).